The Study of High Temperature Oxidation Behavior of Different Microstructures of HVOF Thermally Sprayed Coatings

B. Saeedi[a], A. Sabour Rouhaghdam[a,*]

[a] *Deparatment of Material Science Engineering, Tarbiat Modares University, Tehran, Iran.*

ARTICLE INFO

Article history:

Received 18 Jan. 2014
Accepted 13 Apr. 2014
Available online 15 May 2014

Keywords:

High temperature corrosion
Coatings
Thermal spray
Ni-based alloy

ABSTRACT

Improvement of thermally sprayed coating properties by microstructure modification has been considered as a significant solution. Therefore, in this research the effect of dissolved oxygen content and post heat treatment on the formation and distribution of secondary phase particles, particularly in nano-scale in the coatings during spraying and after that were studied. Ni-5 *wt*% Al powders were sprayed by high velocity oxy-fuel (HVOF) technique under two different oxygen/fuel ratios to achieve different melting states for feedstock materials. As-sprayed coatings were exposed to complementary heat treatment including heating at 1100 °C under inert atmosphere, then furnace cooling to room temperature. The as-sprayed and heat treated coatings were evaluated for high temperature performance. Isothermal oxidation tests were carried out at 950 °C for 100 h. The results showed that depending on the spraying conditions and optimization of the coating microstructure, Ni-based sprayed coatings with low Al content could be utilized as an efficient bond coat or overlay coating.

1. Introduction

The most well-known compositions of efficient high temperature coatings include MCrAlY and Intermetallic alloys. Among intermetallics, Ni-Al alloys have always received more attention due to their unique properties. Although a lot of researches have been carried out on dilute Ni-Al bulk alloys [1], few studies have focused on oxidation behavior of dilute Ni-Al coatings [2]. Particularly, the oxidation behavior of HVOF sprayed Ni-based alloys with low Al content has not been extensively examined compared to MCrAlY coatings.

In the HVOF process, the particles may melt completely or partially, which depends on the flame temperature, the residence time and the melting point of materials and affects the properties of the coatings [3]. It was generally admitted that a key factor to spray oxide free coatings is to avoid complete particle melting and to achieve high particle velocities [4]. On the other hand, high enough melting of powders should provided to assure certain homogeneity level in the coatings [5].

Corresponding author:
E-mail address: sabour01@modares.ac.ir (Alireza Sabour Rouhaghdam).

In order to control the melting state of sprayed materials, the oxygen/fuel ratio was considered as a main parameter to achieve different types of microstructure. The melting degree of powders and the amount of dissolved oxygen during spraying process have significant effects on the formation and distribution of oxides in the coatings. For example, metal oxides residing along the splat boundaries can lower intersplat cohesion, whereas the oxide particles dispersed in the splat or the supersaturated oxygen can also strengthen the splat [6].

In the HVOF-sprayed coatings, the cooling rate of each heated particle upon impact is extremely high (~10^5 K/s), causing splat quenching and resulting in very fine sub-micrometric crystals, metastable supersaturated solid solutions, and even amorphous phases within each splat [7]. Since the as-sprayed coatings mainly consist of supersaturated solid solutions, heat treatments allow the precipitation of the secondary phases which could strengthen the coatings and enhance their characteristics [8].

The aim of this research was to study the relationship between different microstructures obtained by HVOF spraying process and the influence of complementary heat treatment on the resulting properties of Ni-based coatings with low Al content. Isothermal oxidation tests were also carried out on the coatings to determine the resultant properties.

2. Experimental

A type of commercial pre-alloyed, spheroidal gas-atomized Ni–Al powder supplied by "GTV Verschleißschutz GmbH" was used as the starting spray material. The selection of Ni-5 *wt.* % Al was due to its importance as a common and economical bond coat material.

The powders were sprayed onto the stainless steel substrates by a commercial HVOF spray system which consumes propane as a fuel gas. In this study, freestanding coatings were used to exclusively study the behavior of the coatings and prevent the interference of the substrate.

Two different spraying conditions were applied in order to obtain different degrees of melting and in-flight oxidation of powder particles which consequently resulted in two significantly different coating microstructures. Thus, two sets of spraying parameters were selected. The parameters differed in the oxygen/fuel flow rate ratio. The HVOF Spraying parameters are listed in Table 1. These as-sprayed coatings named as NiAl-1 and NiAl-2, were named as NiAl-HT 1 and NiAl-HT 2 after heat treatment . To change the flame temperature, oxygen/fuel ratio was controlled in such a way that the ratio is 74% and 90% of stoichiometric ratio for NiAl-1 and NiAl-2 coatings, respectively. Compressed air jets behind the specimens were also used to cool them during and after spraying.

The specimens were heat treated in a tube furnace under an inert gas atmosphere (Ar + 5%H_2) at 1100 °C for 4 h, followed by furnace cooling under the same atmosphere down to room temperature.

For characterization of the oxidation behavior, the free-standing coatings were subjected to isothermal oxidation treatment at 950 °C for up to 100 h to compare the kinetics of two kinds of coatings. Weight gain of the specimens was measured at specified intervals with a balance with an accuracy of 1×10^{-4} g.

Morphology and microstructure of the powders and coatings were examined by field-emission scanning electron microscopy (FESEM) equipped with energy dispersive spectroscopy (EDS). X-ray diffraction analysis was carried out with Cu K_α radiation (λ = 1.54056 Å) with a step size of 0.026° to characterize the powder and the coatings.

In order to obtain the same surface condition before heat treatment and oxidation test, all the specimens were ground with fine SiC paper to eliminate the oxide layer formed during thermal spraying.

3. Results and Discussion

3. 1. Characterization of powders

Fig 1 shows the morphology of the as-received powders. Original Ni-5Al powders have a spherical shape (typical of gas atomization process). The equiaxed grain structure on the external surface of some powder particles is observed. Size distribution of the powders was in the 10-35 µm range. The average particle

Table 1. HVOF spraying parameters for Ni-5Al coatings

Parameters	NiAl-1	NiAl-2
Propane flow rate (l/min)	60	50
Oxygen flow rate (l/min)	220	225
Powder feed rate (rpm)	450	400
Carrier gas (N_2) flow rate (l/min)	20	20
Spray distance (mm)	280	280

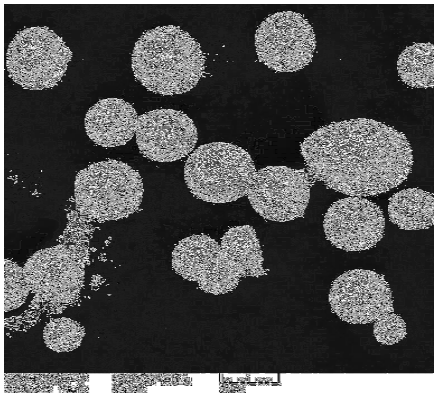

Fig. 1. Morphology of the as-received Ni-5Al powder

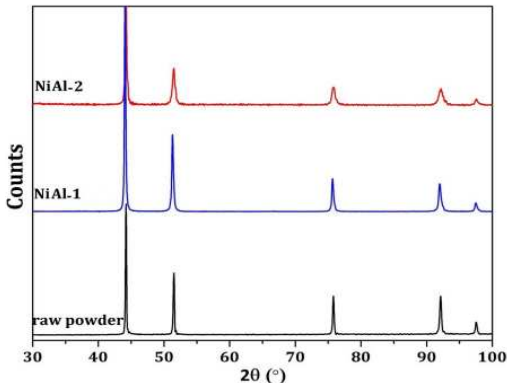

Fig. 2. XRD patterns for powders and as-sprayed coatings

size was determined equal to 21 µm. Composition analysis of the powders included Ni-5.2Al-0.9Fe-0.4Cr (*wt* %). Also, the raw powders contained 0.02 *wt*% oxygen.

According to the XRD patterns (Fig 2), Ni-5Al powders display only *γ*-Ni (FCC solid solution crystal structure). The powders show very sharp *X*-ray diffraction peaks.

3. 2. Characterization of coatings

Figure 3 shows the cross section of the HVOF sprayed coatings. The average thickness of the coatings was in the 300 ± 30 µm range.

As can be seen in Fig 3(a), the NiAl-2 coating shows a typical lamellar structure. This layered structure is generated by flattening of molten particles which influence, along with high velocity, onto the substrate or the already deposited layer. In comparison with NiAl-2 coating with high melting degree of the powders, Fig 3(b) shows a structure containing unmelted powder particles with a semi-spherical shape. The dark veins between the splats in the NiAl-2 coating (Fig 3(a)) and the very thin shell around the particles in NiAl-1 coating (Fig 3(b)) are Al_2O_3. As is well known, the materials during thermal spray suffer oxidation. When spraying in air is carried out, particle oxidation takes place in-flight, at the splat surface and between passes [9]. Therefore, it was tried to deposit the coatings with the acceptable oxide level by controlling the spraying parameters, primarily the oxygen/fuel ratio.

The oxygen content in the coatings was determined to be about 0.18 and 0.29 wt% for NiAl-1 and NiAl-2, respectively. The coating mostly consisted of unmelted particles had the lower oxygen content and showed a little oxidation. In contrast, NiAl-2 coating containing completely melted particles had the higher oxygen and the thin oxide stringers are observed through the coating, due to higher flame temperature and more reaction of the melted particles with oxygen. Since the oxygen content of the initial powders was much lower than the coatings, it could be explained that the oxygen was entrained during spraying process [3].

Spraying condition under fuel-rich mixture for NiAl-1 with 0.74 stoichiometric ratio provided a lower flame temperature; therefore, very low percentage of powders melting occurred. Consequently, such a condition resulted in little oxidation of the powders, just a very thin string of alumina formed around the particles. It is noteworthy that with the aid of compressed air, the velocity of the particles in the flame propelled into the substrate is high enough to compensate for the low melting and

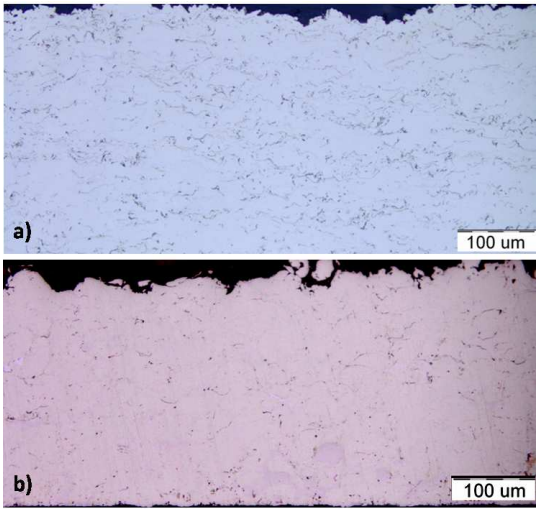

Fig. 3. Optical images of cross section of the as-prayed coatings, (a) NiAl-2 and (b).NiAl-1.

produce a coating with the lowest amount of porosity.

It is presented that the temperature of flame is the highest when the stoichiometric ratio is between 0.9 and 1.0 [10]. As the oxygen/fuel flow rate ratio for NiAl-2 reaches 0.9 of the stoichiometric ratio, it is predictable to produce a dense coating with high percentage of melted powders as a result of a flame jet with higher temperature. Of course, by optimized conditions during both coatings deposition with the moderate melting level, it was tried to avoid thick oxide veins around the particles or between splats.

The XRD patterns of the coatings in Fig 2 show that the matrix was composed of γ-Ni only, whereas there was no peak of Al_2O_3 phase, despite the presence of very thin layers of oxide in the coatings. Its content is probably was lower than the limitation of *X*-ray detection (about 5%). Low amount of the oxide inclusions in the coatings is due to the short flight time of particles and hence reduction of the powder reaction with oxygen. This is one of the preferences of HVOF process [11].

As can be seen in Fig 2, the XRD patterns of the coatings became broader than those of the corresponding powders. Broadening of the peaks resulted from a smaller crystal size and/or existence of microstrains inside crystals [12]. Both phenomena are caused by thermal and kinetic history experienced by powder particles during HVOF spraying. During the spraying, the particles are heated and might impinge on the substrate in unmelted, partially molten or fully molten conditions. Unmelted material may be plastically deformed upon impact, resulting in crystal size reduction and high microstrains inside the crystals. The molten material cools down and solidifies at a fast rate (usually $\geq 10^5$ K/s) upon impact. This cooling rate is much higher than that occurring during the powder manufacturing process [13].

By comparison of XRD patterns of the coatings, the broadening of the peaks for the coating with higher melting degree is clearly observed, while the coating consisting of unmelted particles shows the peaks a little broader than its powder.

It should be noted that quenching stresses arise due to rapid cooling and solidification of the molten particles upon impact. Moreover, during solidification of the sprayed molten droplets, the nucleation rate is higher than that during gas/water atomization, but the crystal growth rate is lower. Thus, finer crystals are found in the sprayed coating than in the original spray powders [13]. The grain size of the coatings estimated by Williamson-Hall method is about 204 nm and 60 nm for NiAl-1 and NiAl-2, respectively. Therefore, smaller grain size and residual stress could be the reasons why higher melting during spraying brought about much broadening of the XRD peaks.

3. 3. Heat Treatment

Morphological variations for the coatings after

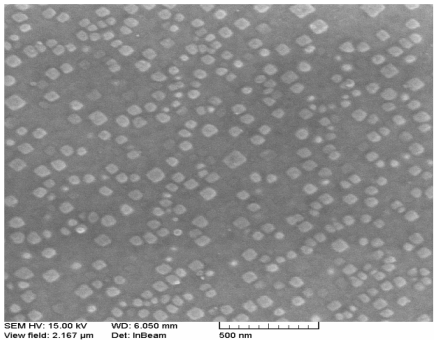

Fig. 4. SEM images of γ'-(Ni_3Al) nanoparticles from the surface of NiAl-HT 1 coating after electroetching.

heat treatment under inert gas were investigated. After annealing, the surface of coatings were ground and polished, and then electroetching with sulphuric acid solution with constant 4 V was carried out in order to reveal the likely precipitates in the alloy.

What occurred in the NiAl-HT 1 coating is summarized in Fig 4. SEM images from top surface of the coating present γ'-(Ni_3Al) nanoparticles as a secondary phase within the unmelted powder particles. The average size of γ' particles is almost 40 nm. These cuboidal precipitates are quite the same as those formed in the slow-cooled Ni-based superalloys [14]. It should be pointed out that the complex metastable state of the as-sprayed coatings which mainly consist of supersaturated solid solutions means that there is a large driving force for microstructural and compositional transformations when exposed to elevated temperatures. The most notable change is the precipitation of secondary fine phases [8, 15].

It is supposed that heat treatment at high enough temperature (1100 °C) for 4 h provided the condition for γ-Ni alloy to transform into an equilibrium solid solution. Then, during slow cooling under inert atmosphere, precipitation of γ'-(Ni_3Al) nanoparticles was facilitated. It is reported that the γ' phase is not a stable phase at high temperature but forms or re-precipitates on cooling below a temperature of approximately 750 °C in NiCoCrAlY coatings [16].

The composition range of γ'-(Ni_3Al) (ordered face-centered cubic (FCC), L12) is 10~35 *at*% Al [17]. On the other hand, low oxygen pressure, high temperature, and low NiO activity promote the formation of NiAl and Ni_3Al phases according to thermodynamic calculations [18]. Since the Al content in NiAl-1 coating remains the same as in the initial composition of the powders (10.64 *at*%) due to low melting degree of the powders and consequently lower consumption of Al as a result of much lower oxidation during spraying process, the formation of γ' could be explained through proper heat treatment.

In spite of what happened within the NiAl-HT 1 coating, the significant change for NiAl-HT 2 coating occurred on its surface. In this situation, the low oxygen partial pressure during heat treatment seems to suppress formation of any other oxides. Therefore, a dense, continuous, and protective Al_2O_3 layer was formed. The cross section of NiAl-HT 2 coating can be seen in Fig 5. Of course, in some regions, mixed oxides were built. As specified by EDS analysis (Fig 5(b)), those regions are combination of Al_2O_3, NiO and $NiAl_2O_4$ (spinel), which indicates the local depletion of Al beneath the surface of the coating. It has been reported that in order to promote the exclusive formation and growth of an adherent and continuous α-Al_2O_3 layer on the metallic bond coating (BC) during service, an initial thermally grown oxide (TGO) is usually grown on the BC surface as a separate processing step could be really efficient. They considered this processing step as a pre-annealing and/or pre-oxidation treatment of the BC prior to deposition of the TBC [19-20].

It is presumed that because of higher amount of melting for NiAl-2 coating, the Al content reduced to below the critical amount for Ni_3Al phase formation. Or even if it was formed, the precipitates would be too fine to be observed even by SEM; TEM would be employed to observe such precipitates.

3. 4. Oxidation behavior of the coatings

Fig 6 shows the kinetic curves of isothermal oxidation of the as-sprayed and heat treated coatings at 950 °C. According to the equation $(\Delta m/A)=k.t^n+C$, the oxidation behavior of all coatings obeys the parabolic law. The parabolic rate constant (k_p) was calculated by plotting the square of weight gain per unit area vs. time. The value of k_P can be used to compare the

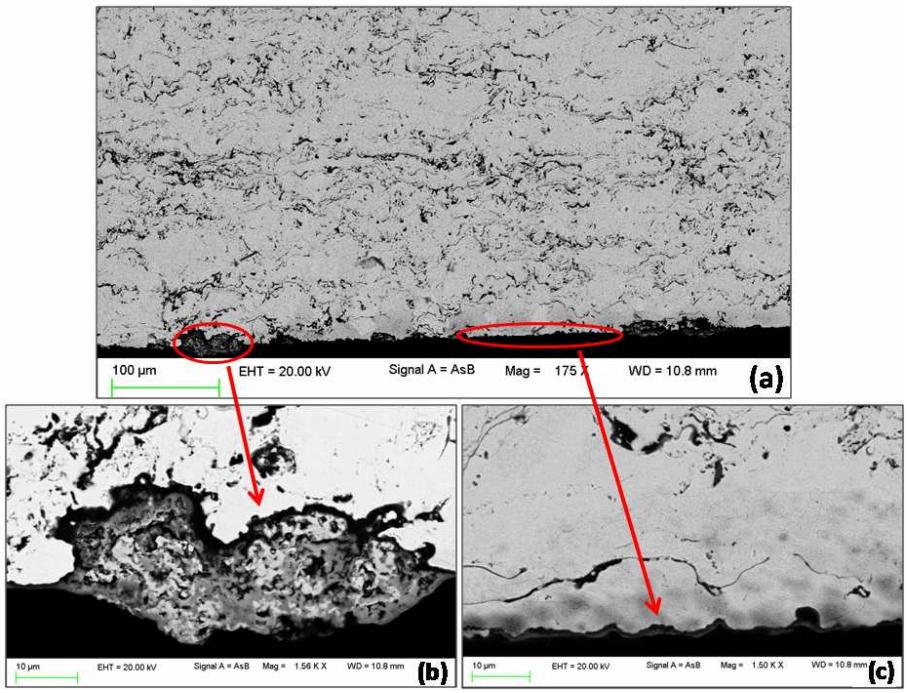

Fig. 5. The cross section of NiAl-HT 2 coating after heat treatment at 1100 °C for 4 h under inert gas.

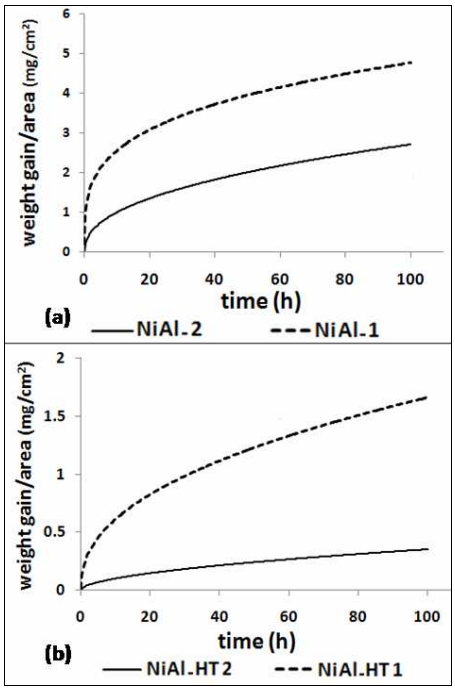

Fig. 6. Weight gain of as-sprayed and heat treated Ni-5Al coatings as a function of time.

oxidation resistance of different materials. In addition, the lower the k_P, the better the oxidation resistance.

From the gradient of the best straight-line fitted to the results of the square of the weight gain per unit area against time, the k_p was determined to be 0.187 and 0.063 mg^2/cm^4h for the NiAl-1, NiAl-2 coatings, respectively. In like manner, the parabolic rate constants calculated for NiAl-HT 1 and NiAl-HT 2 are 0.04 and 0.001 mg^2/cm^4h, respectively.

According to Fig 6(a), the as-sprayed coating

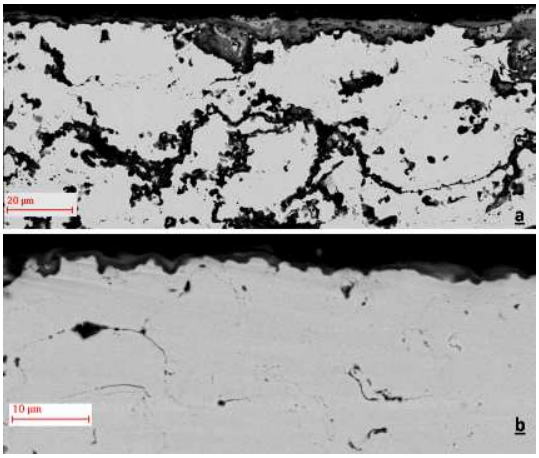

Fig. 7. The cross section of the heat treated coatings after 100 h oxidation: (a) NiAl-HT1 and (b) NiAl-HT2.

with higher melting degree showed more oxidation resistance in spite of more oxides present in the coating, whereas the as-sprayed coating with less melting and the lowest oxides showed higher k_p than NiAl-2 coatings. It is supposed that the coating containing higher unmelted particles experienced lower temperature during spraying, thus only a thin Al_2O_3 layer was generated around the powder particles and prevented the diffusion of oxygen into the particles. Through oxidation, this layer acted as a barrier against the diffusion of Al to reach the surface of the coating and became the protective alumina scale. Actually the elements were trapped inside the particles.

On the other hand, the presence of very thin alumina oxide veins between splats acts as an effective obstacle to the oxygen diffusion into the coating and, more importantly, these finely dispersed α-Al_2O_3 [21] within the NiAl-2 coating favor the nucleation and growth the alumina scale. Because of that, the transient stage of NiAl-2 coating is shorter than that of NiAl-1 coating. The presence of internal oxide was modeled for HVOF sprayed coatings with sufficiently melted particles and showed that the tiny oxides embedded in solidified splats are the oxide inclusions within molten droplets [6].

In comparison with as-sprayed coatings, heat treated coatings showed considerable reduction in parabolic rate constants, particularly for NiAl-HT 2 coating. The difference between the coatings is again attributed to the fact that the convection within the molten droplet will ease the formation of internal oxides, which causes the oxides to be distributed more uniformly through the bulk volume of the particles while oxidation of solid particles (below the melting temperature) during spraying occurs as a shell oxide around the particle [9, 22]. As it was mentioned above, dispersion of fine α-Al_2O_3 particles in the HVOF sprayed coatings with acceptable amount of material melting helps the continuous and protective alumina layer on the coatings. Furthermore, as it was mentioned earlier, the grain size of NiAl-2 coating was smaller than that of NiAl-1 coating. Since the grain boundaries act as easy diffusion paths [2], fast and continuous diffusion and supplying of Al outward to the NiAl-HT 2 coating was provided. It should be mentioned that low pressure of oxygen and high enough temperature during heat treatment are the prerequisites to form the protective α-Al_2O_3 thermally grown oxide.

Despite the homogenous formation and distribution of γ' nanoparticles in NiAl-HT 1 coating, no positive effect was observed on the oxidation behavior of the coating. It seems that the entrapment of γ' nanoparticles inside the powder particles is the main reason. Thus, these nanoparticles did not play any role in supplying Al into the surface of the coating.

Cross section of the heat treated coatings after 100 h oxidation is shown in Fig 7. According to Fig 7(a), in addition to thin alumina layer (dark layer), the massive spinel oxides (gray scales above dark layer) were formed on the NiAl-HT 1 coating. Since spinel oxides are not capable

of protecting the coating against further oxidation, severe internal oxidation is also observed, whereas for NiAl-HT2 coating, a continuous and uniform Al_2O_3 scale is well attached to the coating, as seen in Fig 7(b). Also, internal oxidation of the coating is very little because of excellent protectiveness of alumina layer against diffusion of oxygen toward the NiAl-HT2 coating.

4. Conclusions

In this research, the influence of heat treatment on two different microstructures of Ni-based thermally sprayed coatings with low Al content was studied. The main difference of deposited coatings was the melting degree of powder particles which resulted in different dissolved oxygen content and in-flight oxidation of material during spraying. In order to obtain the different extent of melting, it was focused on the oxygen/fuel flow rate ratio to control the flame temperature. According to the two distinct microstructures, different properties were achieved through heat treatment.

Acknowledgment

The authors would like to thank Dr. Fathollahi and Dr. Shahrabi for their sincere support of this project. The authors also thank Mr. Gholami for his helpful contributions.

References

1. F. S. Pettit, “Oxidation mechanisms for Nickel-Aluminum alloys at temperatures between 900°C and 1300 °C, Trans. Metall. Soc. Aime, Vol. 239, 1967, pp. 1296-1305.
2. D. F. Susan, A. R. Marder, “Oxidation of Ni–Al-base electrodeposited composite coatings. I: oxidation kinetics and morphology at 800°C”, Oxid. Met., Vol. 57, No. 1/2, 2002, pp. 131-157.
3. J. Saaedi, T. W. Coyle, H. Arabi; S. Mirdamadi, J. Mostaghimi, “Effects of HVOF process parameters on the properties of Ni-Cr coatings”, J. Therm. Spray Tech., Vol. 19, No. 3, 2010, pp. 521-530.
4. C. M. Hackett, G. S. Settles, “The Influence of nozzle design on HVOF spray particle velocity and temperature”, Proc. 8th National Thermal Spray Conference, Houston, Texas, 1995, p. 11.
5. W. Brandl, D. Toma, J. Kruger, H. J. Grabke, G. Matthause, “The oxidation behaviour of HVOF thermal-sprayed MCrAlY coatings, Surf. Coat. Techol., Vol. 94-95, 1997, pp. 21-26.
6. S. Deshpande, T. S. Sampath, H. Zhang, “Mechanisms of oxidation and its role in microstructural evolution of metallic thermal spray coatings-Case study for Ni–Al”, Surf. Coat. Technol., Vol. 200, 2006, pp. 5395-5406.
7. J. Y. Cho, S. H. Zhang, T. Y. Cho, J. H. Yoon, Y. K. Joo, S. K. Hur, “The processing optimization and property evaluations of HVOF Co-base alloy T800 coating”, J. Mater. Sci., Vol. 44, 2009, pp. 6348–6355.
8. G. Bolelli, L. Lusvarghi, M. Barletta, “Heat treatment effects on the corrosion resistance of some HVOF-sprayed metal alloy coatings”, Surf. Coat. Technol., Vol. 202, 2008, pp. 4839–4847.
9. P. Fauchais, A. Vardelle, B. Dussoubs, “Quo Vadis Thermal Spraying?”, J. Therm. Spray Tech., Vol. 10, No. 1, 2001, pp. 44-66.
10. G. Zhang, A. F. Kanta, W. Y. Li, H. Liao, C. Coddet, “Characterizations of AMT-200 HVOF NiCrAlY coatings”, Mater. Design, Vol. 30, 2009, pp. 622–627.
11. B. Saeedi, A. Sabour, A. M. Khodami, “Study of microstructure and thermal shock behavior of two types of thermal barrier coatings”, Mater. Corros., Vol. 60, No. 9999, 2009, pp. 1-8.
12. C. Suryanarayana, M. G. Norton, X-Ray Diffraction: A Practical Approach, Springer Science+Business Media, New York 1998.
13. G. Bolelli, L. Lusvarghi, R. Giovanardi, “A comparison between the corrosion resistances of some HVOF-sprayed metal alloy coatings”, Surf. Coat. Technol., Vol. 202, 2008, pp. 4793–4809.
14. M. J. Donachie, S. J. Donachie, Superalloys: A Technical Guide, ASM International, Materials Park, OH, 2002.
15. S. Matthews, M. Hyland, B. James, “Microhardness variation in relation to carbide development in heat treated Cr_3C_2–NiCr thermal spray coatings”, Acta Mater.,

Vol. 51, 2003, pp. 4267–4277.
16. B. G. Mendis, B. Tryon, T. M. Pollock, K. J. Hemker, "Microstructural observations of as-prepared and thermal cycled NiCoCrAlY bond coats", Surf. Coat. Technol., Vol. 201, 2006, pp. 3918–3925.
17. E. Copland, "Solidification behavior of γ'-Ni3Al-containing alloys in the Ni–Al–O system", Acta Mater., Vol. 55, 2007, pp. 4853-4865.
18. Ch. Kuo, W. D. Jehng, Sh. Hsieh, Ch.Chen, "Phase equilibria on Ni–Al interface under low oxygen pressure", J. Alloy. Compd,Vol. 480, 2009, pp. 299–305.
19. T. J. Nijdam, L. P. H. Jeurgens, J. H. Chen, W. G. Sloof, "On the Microstructure of the Initial Oxide Grown by Controlled Annealing and Oxidation on a NiCoCrAlY Bond Coating", Oxid. Met., Vol. 64, No. 5/6, 2005, pp. 355-377.
20. W. R. Chen, X. Wu, B. R. Marple, R. S. Lima, P.C. Patnaik, "Pre-oxidation and TGO growth behaviour of an air-plasma-sprayed thermal barrier coating", Surf. Coat. Technol. Vol. 202, 2008, pp. 3787-3796.
21. D. Toma, W. Brandl, U. Köster, "The Characteristics of alumina scales formed on HVOF-sprayed MCrAlY coatings", Oxid. Met., Vol. 53, No. 1/2, 2000, pp. 125-137.
22. V. V. Sobolev, J. M. Guilemany, "Flattening of droplets and formation of splats in thermal spraying: a review of recent work-part 1", J. Therm. Spray Techn., Vol. 8, No. 1, 1999, pp. 87-101.